Journal Pre-proofs

Epinephrine-Entrapped Chitosan Nanoparticles Covered by Gelatin Nanofibers: A Bi-layer Nano-Biomaterial for Rapid Hemostasis

Mahboubeh Atashgahi, Behnaz Ghaemi, Alireza Valizadeh, Arfa Moshiri, Mohammad hossein Nekoofar, Amir Amani

PII: S0378-5173(21)00880-2
DOI: https://doi.org/10.1016/j.ijpharm.2021.121074
Reference: IJP 121074

To appear in: *International Journal of Pharmaceutics*

Received Date: 14 February 2021
Revised Date: 28 July 2021
Accepted Date: 31 August 2021

Please cite this article as: M. Atashgahi, B. Ghaemi, A. Valizadeh, A. Moshiri, M. hossein Nekoofar, A. Amani, Epinephrine-Entrapped Chitosan Nanoparticles Covered by Gelatin Nanofibers: A Bi-layer Nano-Biomaterial for Rapid Hemostasis, *International Journal of Pharmaceutics* (2021), doi: https://doi.org/10.1016/j.ijpharm.2021.121074

Epinephrine-Entrapped Chitosan Nanoparticles Covered by Gelatin Nanofibers: A Bi-layer Nano-Biomaterial for Rapid Hemostasis

Mahboubeh Atashgahi [a], Behnaz Ghaemi [a#], Alireza Valizadeh [a], Arfa Moshiri [b,c], Mohammad hossein Nekoofar [d,e], Amir Amani [f,g*]

[a] *Department of Medical Nanotechnology, School of Advanced Technologies in Medicine (SATiM), Tehran University of Medical Sciences,1417755469 Tehran, Iran.*

[b] *Gastroenterology and Liver Diseases Research Center, Research Institute for Gastroenterology and Liver Diseases, Shahid Beheshti University of Medical Sciences, 19857-17411 Tehran, Iran.*

[c] *Microbiology Research Center (MRC), Pasteur Institute of Iran, Tehran, Iran*

[d] *Dental Research Center, Dentistry Research Institute, Department of Community Oral Health, School of Dentistry, Tehran University of Medical Sciences, Tehran, Iran.*

[e] *Endodontology Research Group, School of Dentistry, College of Biomedical and Life Sciences, Cardiff University, Cardiff, United Kingdom.*

[f] *Natural Products and Medicinal Plants Research Center, North Khorasan University of Medical Sciences, Bojnurd, Iran.*

[g] *Medical Biomaterial Research Center, Tehran University of Medical Sciences, Tehran, Iran.*

Corresponding Author: *Amir Amani, a.amani@nkums.ac.ir, +98-58-32297097*

#Author's current Affiliation: The Russell H. Morgan Department of Radiology and Radiological Science, Division of MR Research, Johns Hopkins School of Medicine, Baltimore, Maryland 21205, United States

Abstract

Uncontrolled hemorrhage accounts for significant death risk both in trauma and surgery. Various bleeding control techniques have been emerged to augment hemostasis, which still has several limitations and drawbacks. In this study, epinephrine-entrapped chitosan nanoparticles were electrosprayed on a base pad and covered by a gelatin nanofiber layer (E-CS-Gl. Physico-chemical characteristics, hemocompatibility, cytotoxicity, and blood coagulation tests were studied *in-vitro*, and blood coagulation and hemostasis potential tests were performed *in-vivo*. The *in-vitro* results showed that the prepared nano-biomaterial is cytocompatible against HuGu cells. Also, hemocompatibility studies showed that PT and aPTT times did not change in comparison with the controls. Further blood coagulation study indicated that E-CS-Gl provides an ultimate interface to induce red blood cell absorption and aggregation, resulting in augmented blood coagulation. E-CS-Gl also caused rapid clotting in rat models of ruptured femoral artery and liver compared to controls. Findings exhibited that E-CS-Gl is a safe and effective hemostatic agent and provides a new approach for fast and safe hemorrhage control.

Keywords: Chitosan NPs, Epinephrine, Electrospray, Electrospinning; Hemostasis, Biocompatibility.

Introduction

Hemostasis at the surgical site accounts for one of the most challenging issues for surgeons, especially in patients using anticoagulants, where they often require a reduction in dose or discontinuation of the therapy (1, 2). A wide variety of approaches and hemostatic agents have been proposed as solutions for hemostasis due to decreased perfusion and clotting promotion. Mechanical compression of the lesion with gauze is yet considered a straightforward solution for hemostasis. The most challenging drawback of using the mechanical method is that hemostasis time is relatively long. Alternatively, epinephrine is a well-known drug used to reduce hemorrhage and causes pain relief by keeping the co-administrated anesthetic drug in the area (3). Epinephrine is a natural styptic that stimulates general vasoconstriction, resulting in significant inhibition of tissue edema and hemostasis (4). Subcutaneous and topical applications of epinephrine are standard methods associated with immediate control of hemorrhage. Moreover, some hemostasis materials, including natural and synthetic polymers (e.g. collagen, cellulose, chitosan (CS), and gelatin) have been used in hemostatic agents in clinical applications (5, 6). However, there is still a great need for developing new hemostatic materials with high efficacy in an appropriate time.

Owing to high levels of porosity and surface-to-volume ratio, nanoparticles and nanofibers have attracted extensive interests in hemostatic applications (7, 8). In this regard, chitosan nanoparticles and gelatin nanofibers as highly biocompatible materials with antimicrobial and hemostatic properties have been developed (9). The cationic nature of chitosan enables the formation of polyelectrolyte complexes with negatively charged biomolecules to interact with cell membranes and induce platelet aggregation and hemostasis (10). Also, gelatin, a natural biodegradable polymer derived from collagen, is a suitable component for tissue engineering (11), wound healing(12), drug delivery (13), gene therapy (14) purposes. Gelatin has also been applied as a

common component in hemostatic materials. Many studies have shown the synergetic effect of gelatin nanofibers and chitosan NPs on hemostatic activity (15). Literature reported that a combination of chitosan and gelatin improved the blood clotting by forming platelet aggregation in the injury site (16).

In this study, a double layer of epinephrine-entrapped chitosan nanoparticles, covered by an electrospun layer of gelatin nanofibers, was embedded on the surface of gauze pad for rapid hemostasis application. In this regard, chitosan NPs containing epinephrine were prepared through ion gelation and electrosprayed on commercial gauze's surface. Afterward, electrospun gelatin nanofibers were used to cover the surface of the prepared biomaterial. Subsequently, the prepared biomaterial was characterized for composition and *in-vitro* toxicity. The optimized structure was then evaluated for hemostasis applications, *ex-vivo* and *in-vivo*.

Results and Discussion

Preparation and Characterization of E-CS-Gl

Chitosan (CS) NPs were prepared by ion gelation technique, using tripolyphosphate (TPP) as an ionic cross-linker. Obtained results for the charachterization of the epinephrine-loaded chitosan (E-CS) NPs showed a size of ~300-400 nm, which increased by concentration augmentation of epinephrine (Figure S1). At low pH values, the free amino groups of chitosan are protonated, causing electrostatic repulsion between the polymer's chains and increased hydrophilicity of the polymer, thus, enabling polymer solvation (17). Chitosan possesses excellent mucoadhesive properties, resulting from the presence of free hydroxyl and amino groups, allowing the polymer to interact with other molecules by hydrogen and electrostatic bonds (18). In a previous study, the ionic gelation method using low molecular weight chitosan resulted in small CS NPs (93 nm) (19).

Previous reports suggest that CS concentration, molecular weight (20), and temperature (21) may affect the size and size distribution of CS NPs.

Reducing the size and optimizing the shape of E-CS NPs were carried out by electrospraying them on a base pad (Figure 1A). Afterward, gelatin nanofibers were added to the prepared nano-biomaterial surface through the electrospinning method (Figure 1B).

DSC thermograms of epinephrine, CS, and E-CS NPs are shown in Figure 1C. The thermogram of E-CS NPs shows a broad exothermic peak around 312 °C representing its melting temperature, whereas the endothermic peak that occurred at about 50 °C represents water loss from CS (22). The DSC thermograms of chitosan NPs show an exothermic peak at around 280 °C, indicating the melting temperature of CS (23), whereas the endothermic peak that occurred at about 54 °C is due to water loss of chitosan. DSC thermogram of epinephrine shows a peak at around 249 °C, representing drug evaporation temperature. The E-CS NPs show a lower exothermic peak than pure chitosan and pure epinephrine at 280 °C. This phenomenon indicates that a polyelectrolyte complex is formed between CS and epinephrine. Peaks of E-CS NPs shifted from their original positions, indicating an interaction between the drug and the polymer. Collectively, the results suggest that epinephrine was not chemically altered or degraded after being subjected to the electrospray technique (Figure 1C).

SEM analysis reveals that the size of electrosprayed NPs reduced from ~300 nm to ~80 nm with PDI of 0.799 and 0.823, respectively. Results also showed that E-CS NPs prepared with a uniform spherical morphology have a smooth surface with no visible pore (Figure 1D). Furthermore, zeta potential of E-CS NPs was +32.5 mV due to the positive charge of chitosan (at pH < 6.5). Zeta potential can greatly influence particle stability in suspensions through electrostatic repulsion between particles (24).

FTIR spectroscopy was applied to determine the samples' chemical interactions, with representative spectrograms, displayed in Figure S2, which confirm successful loading of epinephrine in the chitosan NPs. These results show a peak of 1600 cm^{-1} in CS, indicating the presence of NH_2 group. After addition of TPP, the signal decreases, which indicates the formation of a chemical bond between NH_2 group of chitosan and TPP. Researchers observed peaks of 1650 cm^{-1} and 1636 cm^{-1} for the amino groups in chitosan and CS-TPP, respectively(25). Another report found that the 1595 cm^{-1} peak of N-H bending vibration shifts to 1540 cm^{-1} in CS-TPP nanoparticles after the addition of TPP (26). The observation of FTIR spectroscopy conforms to the results of the DSC thermograms. Both curves confirmed the formation of a polyelectrolyte complex between chitosan and epinephrine, and no peak representative of covalent interactions could be observed in both curves.

The SEM micrographs indicate that the gelatin nanofibers have a uniform, smooth, and defect-free structure at 13 % wt (Figure 1E). In addition, the mean (SD) diameter of the nanofibers is about 305±50 nm. Also, the SEM study for stability assessment after 40 days showed that the chitosan NPs are stable with the average size of 300±50 nm.

Release profiles of E-CS NPs before and after electrospray were evaluated by suspending the dry nanoparticles in phosphate-buffered solution (PBS, pH 7.4) for five days (Figure S3). Cumulative release of epinephrine reveals a quick burst release within the first 15 min. The epinephrine release profiles from E-CS NPs before and after electrospraying shows ~ 42% and ~ 37% drug release over the first hour, and ~83% and ~ 80% in 20 h, respectively.

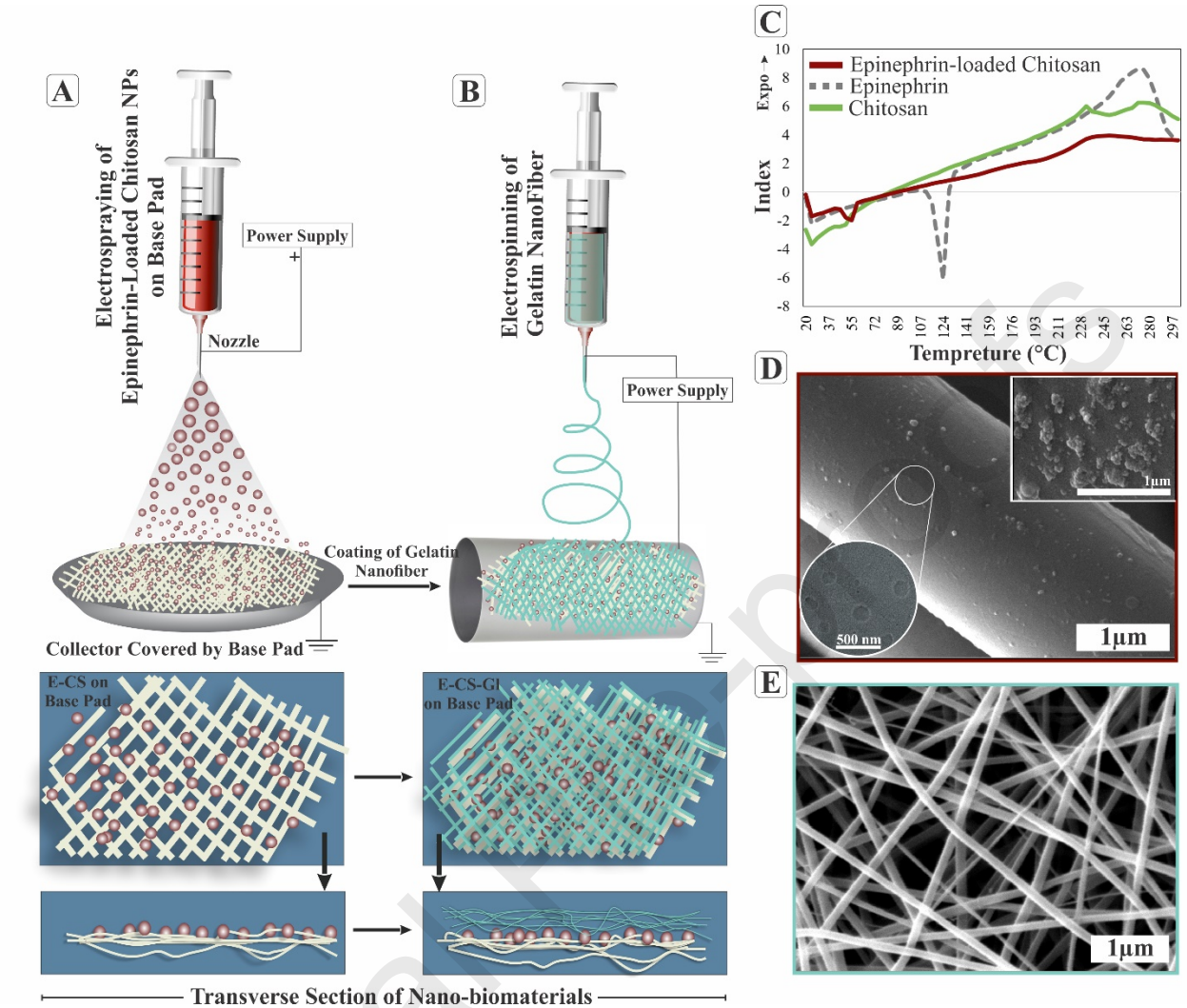

Figure 1. Schematic illustration of the electrospraying of E-CS on the surface of commercial base pad (A), electrospinning of gelatin nanofiber on the E-CS NPs to prepare E-CS-Gl (B), DSC thermogram of prepared E-CS NPs (C), SEM micrograph of electrosprayed E-CS NPs on the surface of base pad (D), formation of Gl nanofiber on the E-CS NPs through electrospinning (E).

In-vitro Cytotoxicity Analysis of E-CS-Gl

In order to evaluate toxicity of E-CS-Gl on HuGu cells, MTT assay was applied for each component in comparison with E-CS-Gl containing epinephrine (300 µg/ml), chitosan (15 %W/V), and gelatin (1.5 %W/V). Results show concentration-dependent toxicity for epinephrine, which increases from 100 µg/ml to 500 µg/ml. Interestingly, although free epinephrine shows about 35% cytotoxicity in a concentration of 300 µg/ml, its encapsulation in chitosan NPs, reduce its toxicity and shows high biocompatibility for E-CS-Gl (Figure 2A). Obtained results for chitosan NPs and gelatin nanofibers do not show any significant cytotoxicity even at the highest concentration applied in this study (Figure 2 B and C). Cytotoxicity of E-CS-Gl prepared with different concentration of components were also evaluated and presented in Figure S4. Results do not reveal any significant toxicity for E-CS-Gl with epinephrine concentration up to 300 µg/ml. Based on the results, it can be clearly stated that E-CS-Gl exhibits low cytotoxicity. It has been reported that CS-TPP nanoparticles were less toxic than other cationic polymers such as poly-lysine and polyethyleneimine *in vivo* and *in vitro* (27, 28). Qi et al. reported cytotoxicity for chitosan particles at concentrations above 16 µg/ml towards MGC803 cells (24 h incubation) (29). Koudehi et al. reported no toxicity of gelatin toward CHO cells after 72 h incubation (30). Because of the nontoxic nature of E-CS NPs and gelatin nanofibers, especially at prepared concentrations, this nano-biomaterial could pave the way to be used in biomedical applications.

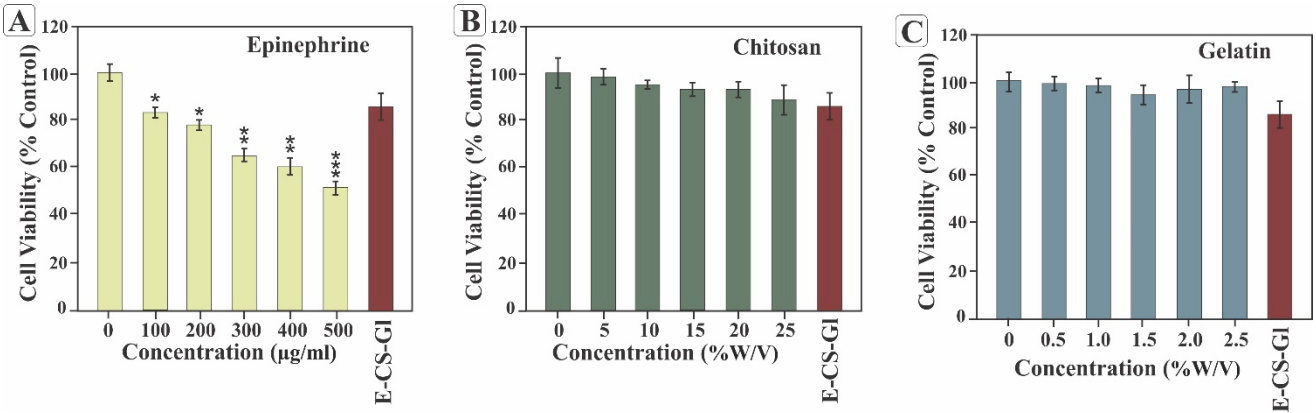

Figure 2. Cytotoxicity assessment for epinephrine (A), chitosan NPs (B), and gelatin nanofibers (C), in comparison with E-CS-Gl. All samples are compared with untreated control, and * , ** and *** are referred to $P \leq 0.05$, $P \leq 0.01$ and $P \leq 0.001$ respectively.

In-vitro Hemolytic Studies

A fundamental assay in determining safety of a blood-contacting biomaterial is evaluating its hemolytic potential (31). Accordingly, the effect of E-CS-Gl on hemolysis of erythrocytes was assessed in this study. Obtained results for hemolysis of chitosan NPs, E-CS NPs, Gl nanofibers, and E-CS-Gl in comparison with PBS are shown in Table 1. The hemolysis ratio increased from 2.1% for CS NP to 3.4% for E-CS-Gl. According to ASTM standard of F756, hemoglobin release of 0–2%, 2–5%, and >5% is classified as nonhemolytic, slightly hemolytic, and hemolytic, respectively (32).

Table 1. Hemolysis evaluation of E-CS-Gl components (N=6)

SAMPLE	COMPOSITION	HEMOLYSIS
CS NP	Chitosan: 15%	2.1 % ± 0.1
Gelatin Nanofibers (13 %)	Gelatin: 1.5%	3.1 % ±0.2
E-CS NP	Chitosan:15%, Epinephrine: 300 µg/ml	3 % ±0.6
E-CS-Gl	Chitosan:15%, Gelatin 1.5%, Epinephrine: 300 µg/ml	3.4% ±0.5
PBS		1 % ±0.1

***In-Vitro* Blood Clotting Evaluation.**

Fluid absorption capacity is the ability of different dressings to absorb normal saline and citrated whole blood, which was analyzed for base pad covered by E-CS NPs and E-CS-Gl in comparison with bare base pad and market patch (Gelfoam®) (Figure 3A). Normal saline (NS) and whole blood (WB) absorption by E-CS-Gl was 270% and 300%, while the market patch absorbed 200% and 210% of the NS and WB sample, respectively. It should be noted that comparing absorption ratio in base pad containing E-CS NPs with that of E-CS-Gl shows that 1.5% gelatin nanofiber accounts for about 100% more liquid absorption in E-CS-Gl. Also, the whole blood clotting assay in Figure 3B shows the highest E-CS-Gl capacity for blood clotting compared to other groups.

The blood clotting time of the tested biomaterials was measured by the clotting time of citrated human blood. Obtained results showed a significant decrease to about 20 seconds following E-CS-Gl's application, while this time for base pad was about 110 seconds (Figure 3C). Also, blood clotting time for the base pad containing E-CS NPs and market patch reduced about 52 and 70 seconds, respectively, compared with the base pad.

Afterward, agglutination of red blood cells (RBCs) and platelets was evaluated by applying a fresh blood sample on the surface of E-CS-Gl (Figure 3D). Results showed that E-CS-Gl activates agglutination and coagulation procedures, which results in blood clotting immediately. Also, Figure 3E shows a microscopic image of the hemostatic plug formation on the surface of E-CS-Gl.

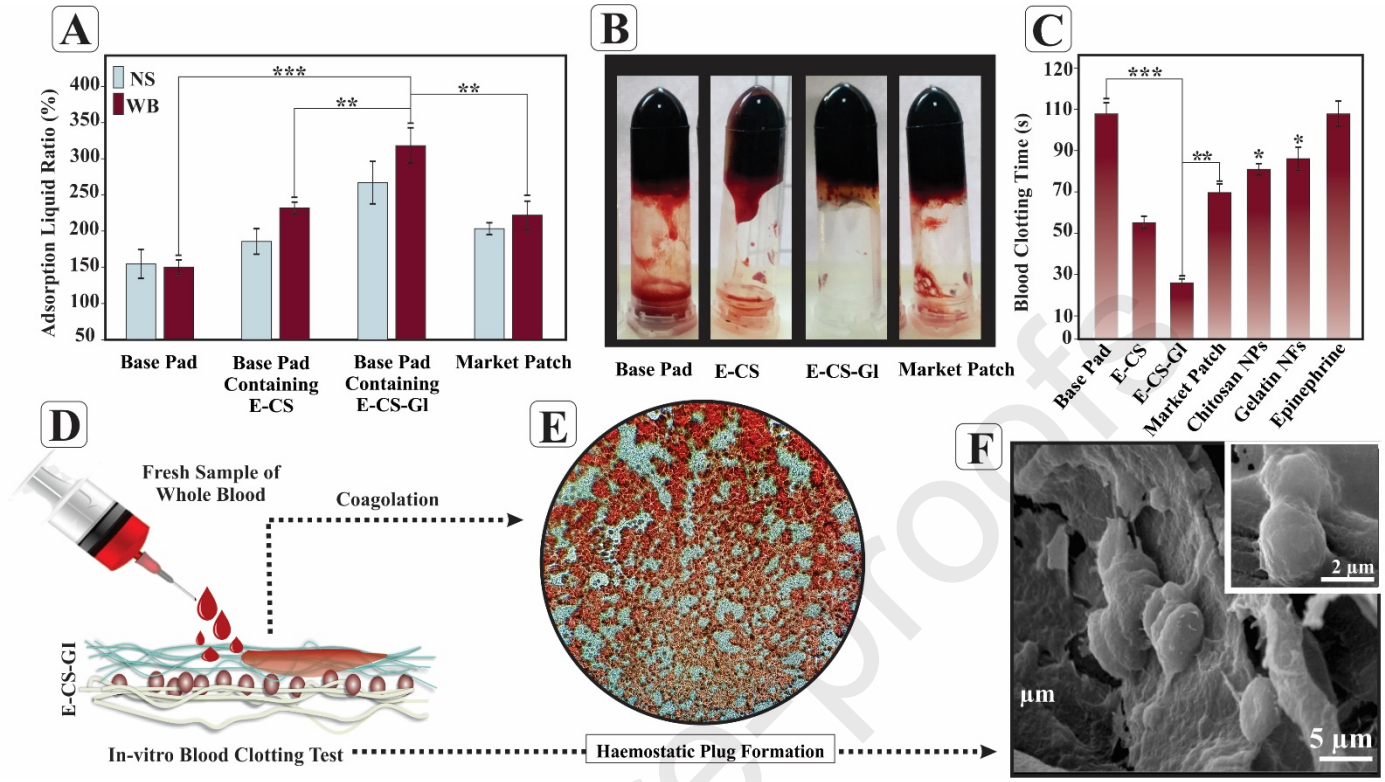

Figure 3. *In-vitro* blood clotting of E-CS-Gl (base pad containing E-CS-Gl). Liquid adsorption ratio (whole citrated blood; WB and normal saline; NS) of hemostatic material (A), whole blood clotting assay for the base pad, base pad containing E-CS NPs (E-CS), base pad containing E-CS-Gl (E-CS-Gl) in comparison with market patch (Gelfome®) (B), blood clotting time of the base pad containing the biomaterials understudy (C), a schematic illustration of coagulation procedure (D), morphology of coagulation of fresh blood sample on E-CS-Gl with optical microscopy (E), and SEM micrograph of hemostatic plug formation on E-CS-Gl (F).

To study the platelet/RBC aggregation mechanism, the effects of epinephrine, chitosan, gelatin and E-CS-Gl on platelet activation and thrombin generation were evaluated through SEM analysis (Figure 4).

SEM micrographs in Figures 3F and 4 show that RBCs have substantially adhered to the surface of the nano-biomaterial, forming a thrombus followed by platelet activation (35). The results show that chitosan NPs and gelatin nanofibers activate coagulation mechanisms through platelet activation, while epinephrine alone does not appear to activate platelets, nor aggregate RBCs. Literature shows that chitosan NPs protonate amine groups, absorbing residues with negative charge on RBC membranes, resulting in effective hemagglutination (33). Also, chitosan can absorb fibrinogen and plasma proteins, elevating platelet activation and RBC aggregation (34). Previous studies on biomaterials reported activation of platelets and coagulation for carboxylated and amidated surfaces, as observed for chitosan in our study (38). Moreover, gelatin activates the contact cascade, which decreases both the time lag for initial thrombin development as well as the time to generate thrombin (15), causing a stable clot which results in hemostasis. Our findings also showed a round morphology for the platelets in contact with base pad containing epinephrine, showing no interaction between the platelets and epinephrine (36, 37).

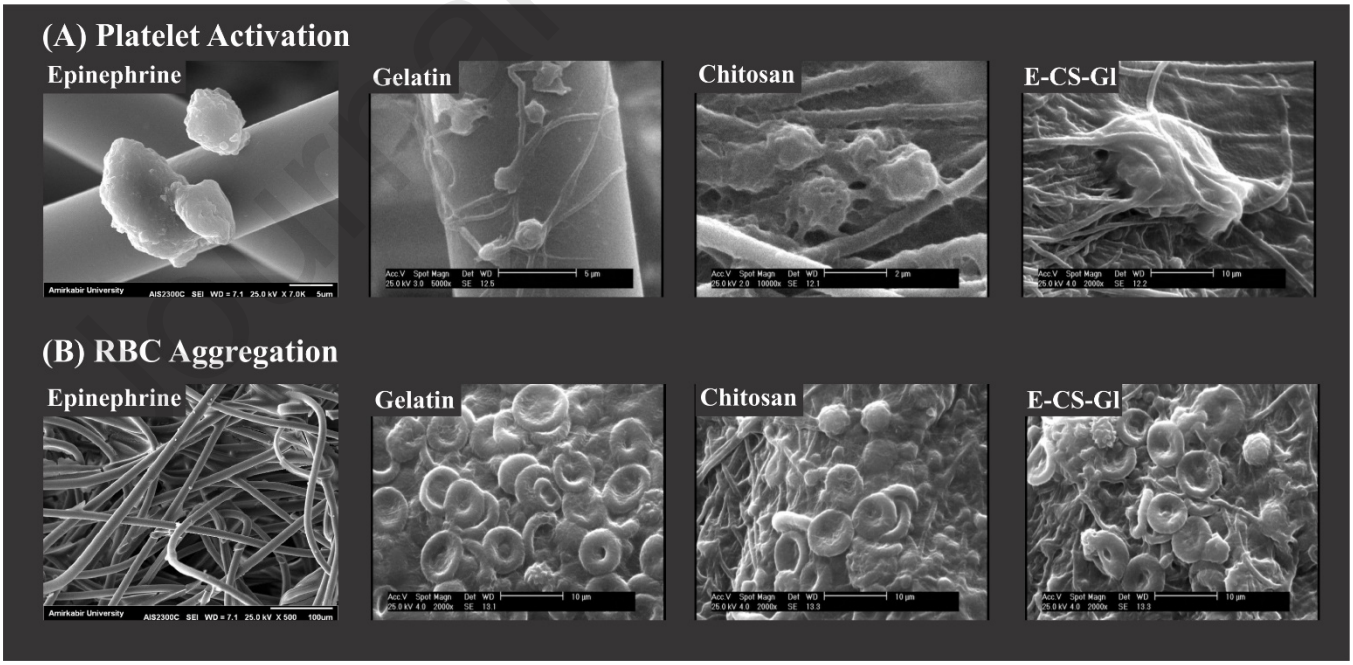

Figure 4. SEM images of platelets and RBCs in contact with base pad containing epinephrine, gelatin, chitosan, and E-CS-Gl.

Plasma Activated Partial Thromboplastin Time (aPTT) and Prothrombin Time (PT)

The coagulation pathway involves a series of proteolytic reactions (including intrinsic and extrinsic pathways), which result in the formation of a fibrin clot. Evaluation of anticoagulant activity based on plasma coagulation has been recognized as a standard test to estimate blood compatibility of a biomaterial (31). The PT assay shows deficiencies of factors II, V, VII, X, and fibrinogen, while the PTT assay detects lacks factors VIII, IX, and XI and fibrinogen. The results of PT and aPTT analyses are shown in Figure 5. The results showed a significant decrease (about 20%) in PT after applying E-CS-Gl, while aPTT did not significantly change. Also studies were done for Epinephrine, chitosan and gelatin have not shown any significant effect on PT and PTT time.

Literature demonstrated that chitosan's hemostatic activity is due to the electrostatic interactions between the positively charged chitosan polymers with the negatively charged RBCs (39, 40). For materials with negative surface charge, intrinsic blood coagulation is promoted by activating coagulant factors XI and XII, and cofactors HWK-kininogen and prekallikrein (41). Also, gelatin nanofiber prepares a contact platform for aggregation of thrombin which synergistically results in faster coagulation followed by hemostasis.

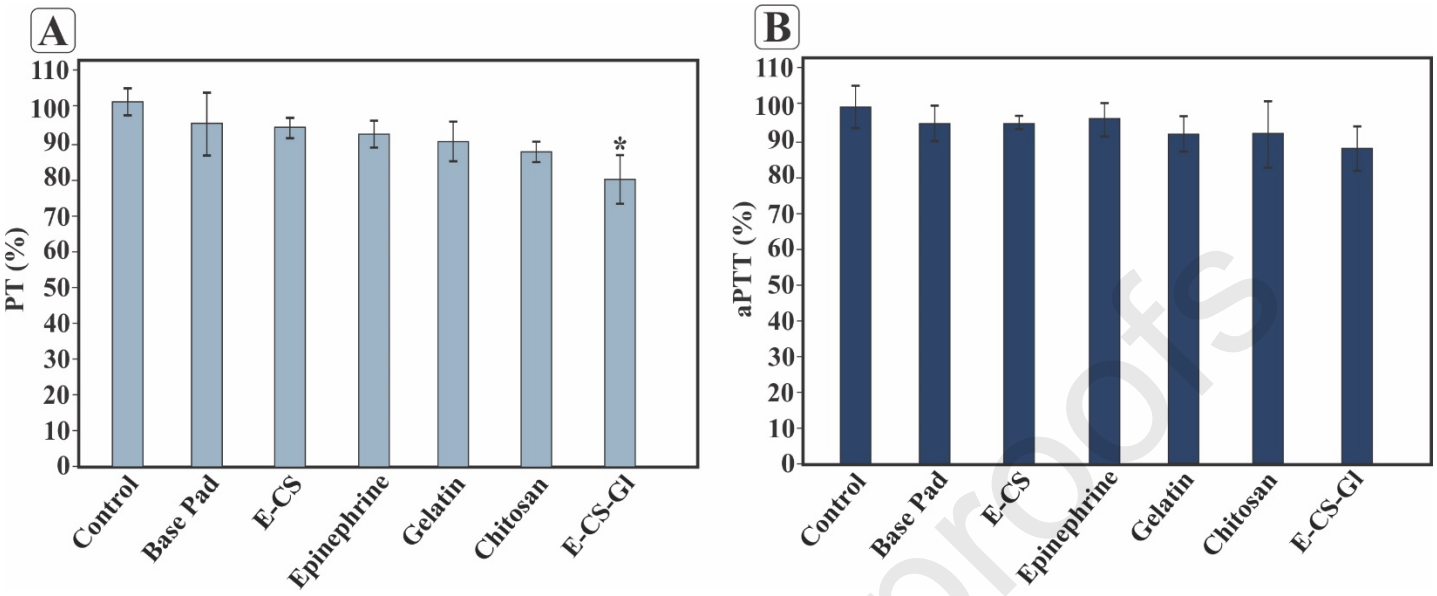

Figure 5. Analyses of PT and aPTT after applying base pad, base pad containing epinephrine, gelatin, chitosan, E-CS and E-CS-Gl.

In-Vivo Hemostatic Performance of E-CS-Gl

Total incision of the femoral artery and liver rupture were employed to evaluate the *in-vivo* hemostatic effect of E-CS-Gl compared to controls.

Ruptured Femoral Artery Model. Bleeding started with incision of the femoral artery, and the homeostatic materials were applied immediately, then, bleeding duration was checked for up to 5 min (Figure 6A). From the findings, in the blank group, the bleeding was stopped after 247 s. Animals receiving base pad and base pad containing E-CS NPs also bled for 203 s and 163 s, respectively (Figure 6B). Furthermore, base pad containing free epinephrine showed 97 s decrease in hemostatic time in comparison with blank, reaching 160 s. Meanwhile, the shortest bleeding time was achieved by applying base pad containing E-CS-Gl (99 s), followed by market patch as commercial control (140 s). Lower blood loss might be due to the gelatin nanofibers' tissue

adhesive nature in the developed nano-biomaterial (42). Results are in accordance with previous studies that reported chitosan's effect to stop bleeding (43, 44). Researches have shown that *in-vitro* and *in-vivo* blood clotting efficiency of gelatin-blended-chitosan nanofiber mats is superior to chitosan nanofibers (15). Researches indicate that hydrophilic gelatin-chitosan nanofiber mats yields synergistic effects that improve hemostatic and promote wound repair (15). Previous reports on clinical study showed that high dose of gelatin causes hemostasis through platelet adhesion (45).

Ruptured Liver Model. In the liver wound model, the liver's left lateral lobe was removed, with a resulting wound surface area of 2×0.5 cm^2 onto which different treatments were applied (Figure 6C). Control animals with no treatment continued to bleed for 104 s, while 50% of the animals were still bleeding at the end of the experiment. Animals receiving base pad and E-CS NPs incorporated base pad also bled for 97 s and 75 s, respectively. Also, the base pad containing free epinephrine showed a decrease in bleeding time (70 s). Results for E-CS-Gl and market patch showed a bleeding time of 33 s and 54 s, respectively (Figure 6D).

Literature showed that epinephrine causes intraoperative hemostasis and hemodynamic changes due to its vasoconstriction properties (46). Furthermore, chitosan can easily adhere to the area of injury, improving vasoconstriction, followed by activating erythrocytes, clotting factors, and platelets with appropriate mucoadhesive property (47, 48). Also, hemadsorption induced by epinephrine and chitosan triggers RBCs' aggregation and clotting (49, 50). Therefore, a combination of epinephrine and chitosan can improve the vasoconstriction, resulting in a decreased in blood flow in the lesion area. Moreover, the fast fluid absorption of gelatin nanofiber may enhance platelet concentration and clotting factors, resulting in shortening the time for thrombin generation (51). Accordingly, *in-vivo* hemostasis experiments demonstrated that the combination

of epinephrine-entrapped chitosan NPs and gelatin nanofibers improved the hemostatic advantages of both materials provided efficient bleeding control.

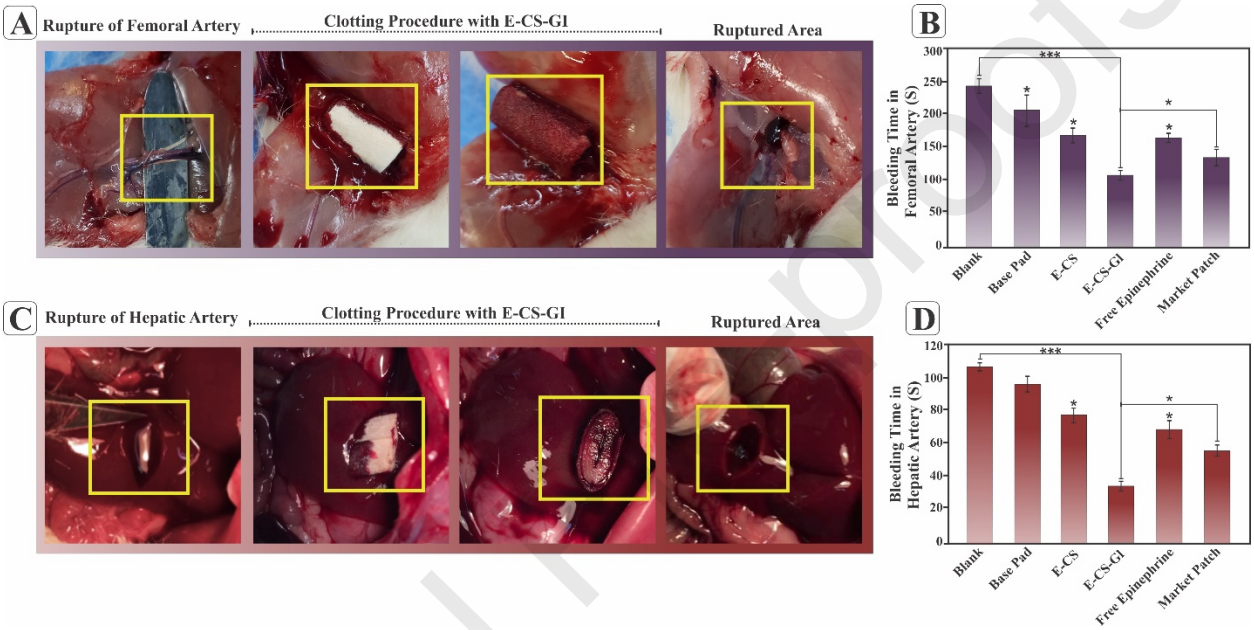

Figure 6. Total incision of femoral artery and hemostasis procedure after applying base pad containing E-CS-Gl (E-CS-Gl) (A), bleeding time in femoral artery injury upon application of different treatments (B), liver rupture and hemostasis procedure when using of a base pad containing E-CS-Gl (C) and bleeding time in liver injury upon application of base pad, base pad containing E-CS NPs (E-CS), base pad containing E-CS-Gl (E-CS-Gl) in comparison with free epinephrine and market patch (D).

Conclusion

In this study, electrosprayed epinephrine-entrapped chitosan NPs on the base pad was covered by gelatin nanofibers and successfully used as hemostatic nano-biomaterial. The prepared nano-

biomaterial showed significant biocompatibility, which is critical for a hemostatic agent. According to our *in-vivo* findings, a base pad containing E-CS-Gl has a great hemostatic potential in the femoral artery and liver injury, created in a rat model with lower blood loss and controlled bleeding. It should be emphasizing that this study determined the hemostatic property of epinephrine-entrapped chitosan and provided an alternative approach for hemorrhage control by electrospinning gelatin nanofibers on the surface of the nano-biomaterial.

Acknowledgment

This study was supported by Tehran University of Medical Science (TUMS).

Author Statement

M. Atashgahi: Conceptualization, Methodology, Formal Analysis. **B. Ghaemi**: Data curation, Writing- Original draft preparation, Visualization, Software. **A. Valizadeh:** Methodology, Formal Analysis. **A. Moshiri:** Writing- Original draft preparation, Writing- Reviewing and Editing, Visualization. **M. H. Nekoofar:** Conceptualization, Validation, Supervision. **A. Amani:** Conceptualization, Writing-Reviewing and Editing, Investigation, Supervision.

Supporting Information

Material and Methods, Dynamic light scattering (DLS) of prepared E-CS NPs, FTIR spectrum of prepared NP and component, the release profile of epinephrine-entrapped chitosan NPs and toxicity assessment of base pad containing E-CS-Gl with different concentration of component.

Disclosure

The authors have no conflict of interest to declare.

References

1. Zanon E, Martinelli F, Bacci C, Cordioli G, Girolami A. Safety of dental extraction among consecutive patients on oral anticoagulant treatment managed using a specific dental management protocol. Blood coagulation & fibrinolysis. 2003;14(1):27-30.
2. Alexander RE. Dental extraction wound management: a case against medicating postextraction sockets. Journal of Oral and Maxillofacial Surgery. 2000;58(5):538-51.
3. Kaise M, Nagata N, Ishii N, Omori J, Goto O, Iwakiri K. Epidemiology of colonic diverticula and recent advances in the management of colonic diverticular bleeding. Digestive Endoscopy. 2019.
4. di Lena F. Hemostatic polymers: the concept, state of the art and perspectives. Journal of Materials Chemistry B. 2014;2(23):3567-77.
5. Zheng C, Liu X, Luo X, Zheng M, Wang X, Dan W, et al. Development of a novel bio-inspired "cotton-like" collagen aggregate/chitin based biomaterial with a biomimetic 3D microstructure for efficient hemostasis and tissue repair. Journal of Materials Chemistry B. 2019;7(46):7338-50.
6. Sun Z, Chen X, Ma X, Cui X, Yi Z, Li X. Cellulose/keratin–catechin nanocomposite hydrogel for wound hemostasis. Journal of Materials Chemistry B. 2018;6(38):6133-41.
7. Nakielski P, Pierini F. Blood interactions with nano-and microfibers: recent advances, challenges and applications in nano-and microfibrous hemostatic agents. Acta biomaterialia. 2019;84:63-76.
8. Wang XX, Liu Q, Sui JX, Ramakrishna S, Yu M, Zhou Y, et al. Recent Advances in Hemostasis at the Nanoscale. Advanced healthcare materials. 2019;8(23):1900823.
9. Leonhardt EE, Kang N, Hamad MA, Wooley KL, Elsabahy M. Absorbable hemostatic hydrogels comprising composites of sacrificial templates and honeycomb-like nanofibrous mats of chitosan. Nature communications. 2019;10(1):2307.
10. Muthiah Pillai NS, Eswar K, Amirthalingam S, Mony U, Kerala Varma P, Jayakumar R. Injectable Nano Whitlockite Incorporated Chitosan Hydrogel for Effective Hemostasis. ACS Applied Bio Materials. 2019;2(2):865-73.
11. Yang G, Lin H, Rothrauff BB, Yu S, Tuan RS. Multilayered polycaprolactone/gelatin fiber-hydrogel composite for tendon tissue engineering. Acta biomaterialia. 2016;35:68-76.
12. Dong Y, Rodrigues M, Li X, Kwon SH, Kosaric N, Khong S, et al. Injectable and tunable gelatin hydrogels enhance stem cell retention and improve cutaneous wound healing. Advanced Functional Materials. 2017;27(24):1606619.
13. Luo Z, Sun W, Fang J, Lee K, Li S, Gu Z, et al. Biodegradable Gelatin Methacryloyl Microneedles for Transdermal Drug Delivery. Advanced healthcare materials. 2019;8(3):1801054.
14. Abozeid SM, Hathout RM, Abou-Aisha K. Silencing of the metastasis-linked gene, AEG-1, using siRNA-loaded cholamine surface-modified gelatin nanoparticles in the breast carcinoma cell line MCF-7. Colloids and Surfaces B: Biointerfaces. 2016;145:607-16.
15. Gu BK, Park SJ, Kim MS, Lee YJ, Kim J-I, Kim C-H. Gelatin blending and sonication of chitosan nanofiber mats produce synergistic effects on hemostatic functions. International journal of biological macromolecules. 2016;82:89-96.
16. Li H, Cheng F, Gao S, Wu Z, Dong L, Lin S, et al. Preparation, characterization, antibacterial properties, and hemostatic evaluation of ibuprofen-loaded chitosan/gelatin composite films. Journal of Applied Polymer Science. 2017;134(42):45441.
17. Al-Nemrawi N, Alsharif S, Dave R. Preparation of chitosan-TPP nanoparticles: the influence of chitosan polymeric properties and formulation variables. International Journal of Applied Pharmaceutics. 2018;10(5):60-5.
18. Xu J, Tam M, Samaei S, Lerouge S, Barralet J, Stevenson MM, et al. Mucoadhesive chitosan hydrogels as rectal drug delivery vessels to treat ulcerative colitis. Acta biomaterialia. 2017;48:247-57.

19. Wu J, Wang Y, Yang H, Liu X, Lu Z. Preparation and biological activity studies of resveratrol loaded ionically cross-linked chitosan-TPP nanoparticles. Carbohydrate polymers. 2017;175:170-7.
20. Jonassen H, Kjøniksen A-L, Hiorth M. Stability of chitosan nanoparticles cross-linked with tripolyphosphate. Biomacromolecules. 2012;13(11):3747-56.
21. Agarwal M, Agarwal MK, Shrivastav N, Pandey S, Das R, Gaur P. Preparation of chitosan nanoparticles and their in-vitro characterization. International journal of life science scientific research. 2018;4(2):1713-20.
22. Echazú MIA, Olivetti CE, Anesini C, Perez CJ, Alvarez GS, Desimone MF. Development and evaluation of thymol-chitosan hydrogels with antimicrobial-antioxidant activity for oral local delivery. Materials Science and Engineering: C. 2017;81:588-96.
23. Piyakulawat P, Praphairaksit N, Chantarasiri N, Muangsin N. Preparation and evaluation of chitosan/carrageenan beads for controlled release of sodium diclofenac. Aaps PharmSciTech. 2007;8(4):120.
24. Gan Q, Wang T, Cochrane C, McCarron P. Modulation of surface charge, particle size and morphological properties of chitosan–TPP nanoparticles intended for gene delivery. Colloids and Surfaces B: Biointerfaces. 2005;44(2-3):65-73.
25. Dai Lam T, Hoang VD, Le Ngoc Lien NNT, Dien PG. Synthesis and characterization of chitosan nanoparticles used as drug carrier. Journal of Chemistry. 2006;44(1):105-9.
26. Mohammadpourdounighi N, Behfar A, Ezabadi A, Zolfagharian H, Heydari M. Preparation of chitosan nanoparticles containing Naja naja oxiana snake venom. Nanomedicine: Nanotechnology, Biology and Medicine. 2010;6(1):137-43.
27. Carreno-Gomez B, Duncan R. Evaluation of the biological properties of soluble chitosan and chitosan microspheres. International Journal of Pharmaceutics. 1997;148(2):231-40.
28. Burke AR, Singh RN, Carroll DL, Owen JD, Kock ND, D'Agostino Jr R, et al. Determinants of the thrombogenic potential of multiwalled carbon nanotubes. Biomaterials. 2011;32(26):5970-8.
29. Qi L-F, Xu Z-R, Li Y, Jiang X, Han X-Y. In vitro effects of chitosan nanoparticles on proliferation of human gastric carcinoma cell line MGC803 cells. World Journal of Gastroenterology: WJG. 2005;11(33):5136.
30. Masoumeh FK, Kamali M, Nourani MR, Ali IFA. Evaluation the cytotoxic/viability effect of gelatin/bioactive glass conduits by MTT assay. Journal of Applied Tissue Engineering. 2014;1(1):22-5.
31. Horakova J, Mikes P, Saman A, Svarcova T, Jencova V, Suchy T, et al. Comprehensive assessment of electrospun scaffolds hemocompatibility. Materials Science and Engineering: C. 2018;82:330-5.
32. Dobrovolskaia MA, Clogston JD, Neun BW, Hall JB, Patri AK, McNeil SE. Method for analysis of nanoparticle hemolytic properties in vitro. Nano letters. 2008;8(8):2180-7.
33. Klokkevold PR, Fukayama H, Sung EC, Bertolami CN. The effect of chitosan (poly-N-acetyl glucosamine) on lingual hemostasis in heparinized rabbits. Journal of oral and maxillofacial surgery. 1999;57(1):49-52.
34. Yang J, Tian F, Wang Z, Wang Q, Zeng YJ, Chen SQ. Effect of chitosan molecular weight and deacetylation degree on hemostasis. Journal of Biomedical Materials Research Part B: Applied Biomaterials. 2008;84(1):131-7.
35. Osorio M, Cañas A, Puerta J, Díaz L, Naranjo T, Ortiz I, et al. Ex Vivo and In Vivo Biocompatibility Assessment (Blood and Tissue) of Three-Dimensional bacterial nanocellulose biomaterials for soft tissue implants. Scientific reports. 2019;9(1):1-14.
36. Herklotz M, Hanke J, Hänsel S, Drichel J, Marx M, Maitz MF, et al. Biomaterials trigger endothelial cell activation when co-incubated with human whole blood. Biomaterials. 2016;104:258-68.
37. Thorson TJ, Gurlin RE, Botvinick EL, Mohraz A. Bijel-templated implantable biomaterials for enhancing tissue integration and vascularization. Acta biomaterialia. 2019.

38. Sperling C, Maitz MF, Grasso S, Werner C, Kanse SM. A positively charged surface triggers coagulation activation through factor VII activating protease (FSAP). ACS applied materials & interfaces. 2017;9(46):40107-16.
39. Ong S-Y, Wu J, Moochhala SM, Tan M-H, Lu J. Development of a chitosan-based wound dressing with improved hemostatic and antimicrobial properties. Biomaterials. 2008;29(32):4323-32.
40. Li D, Nie W, Chen L, Miao Y, Zhang X, Chen F, et al. Fabrication of curcumin-loaded mesoporous silica incorporated polyvinyl pyrrolidone nanofibers for rapid hemostasis and antibacterial treatment. RSC Advances. 2017;7(13):7973-82.
41. Huang S, Engberg AE, Jonsson N, Sandholm K, Nicholls IA, Mollnes TE, et al. Reciprocal relationship between contact and complement system activation on artificial polymers exposed to whole human blood. Biomaterials. 2016;77:111-9.
42. Rahimnejad M, Zhong W. Mussel-inspired hydrogel tissue adhesives for wound closure. RSC advances. 2017;7(75):47380-96.
43. Chan LW, Kim CH, Wang X, Pun SH, White NJ, Kim TH. PolySTAT-modified chitosan gauzes for improved hemostasis in external hemorrhage. Acta biomaterialia. 2016;31:178-85.
44. Feng C, Li J, Wu GS, Mu YZ, Kong M, Jiang CQ, et al. Chitosan-coated diatom silica as hemostatic agent for hemorrhage control. ACS applied materials & interfaces. 2016;8(50):34234-43.
45. Tabuchi N, de Haan J, Huet RCG, Boonstra PW, van Oeveren W. Gelatin use impairs platelet adhesion during cardiac surgery. Thrombosis and haemostasis. 1995;74(12):1447-51.
46. Shoroghi M, Sandrolsadat SH, Razzaghi M, Farahbakhsh F, Sheikhvatan M, Sheikhfathollahi M, et al. Effect of different epinephrine concentrations on local bleeding and hemodynamics during dermatologic surgery. Acta dermatovenerologica Croatica. 2008;16(4):0-.
47. Ikeda Y, Young LH, Vournakis JN, Lefer AM. Vascular effects of poly-N-acetylglucosamine in isolated rat aortic rings. Journal of Surgical Research. 2002;102(2):215-20.
48. Kheirabadi BS, Edens JW, Terrazas IB, Estep JS, Klemcke HG, Dubick MA, et al. Comparison of new hemostatic granules/powders with currently deployed hemostatic products in a lethal model of extremity arterial hemorrhage in swine. Journal of Trauma and Acute Care Surgery. 2009;66(2):316-28.
49. Lee F-Y, Lee D, Lee T-C, Chen J-K, Wu R-C, Liu K-C, et al. Fabrication of Multi-Layered Lidocaine and Epinephrine-Eluting PLGA/Collagen Nanofibers: In Vitro and In Vivo Study. Polymers. 2017;9(9):416.
50. D'hondt A, Haentjens L, Brassart N, Flamme F, Preiser J-C. Uncontrolled bleeding of the gastrointestinal tract. Current opinion in critical care. 2017;23(6):549-55.

51. Chen S, Carlson MA, Zhang YS, Hu Y, Xie J. Fabrication of injectable and superelastic nanofiber rectangle matrices ("peanuts") and their potential applications in hemostasis. Biomaterials. 2018;179:46-59.

Mahboubeh Atashgahi: Investigation, Methodology, Writing - Original Draft

Behnaz Ghaemi: Methodology, Formal analysis, Writing - Review & Editing

Alireza Valizadeh: Methodology, Writing - Review & Editing

Arfa Moshiri: Methodology, Writing - Review & Editing

Mohammad hossein Nekoofar: Conceptualization, Supervision, Writing - Review & Editing

Amir Amani: Methodology, Conceptualization, Validation, Writing - Review & Editing, Supervision, Project administration, Project administration

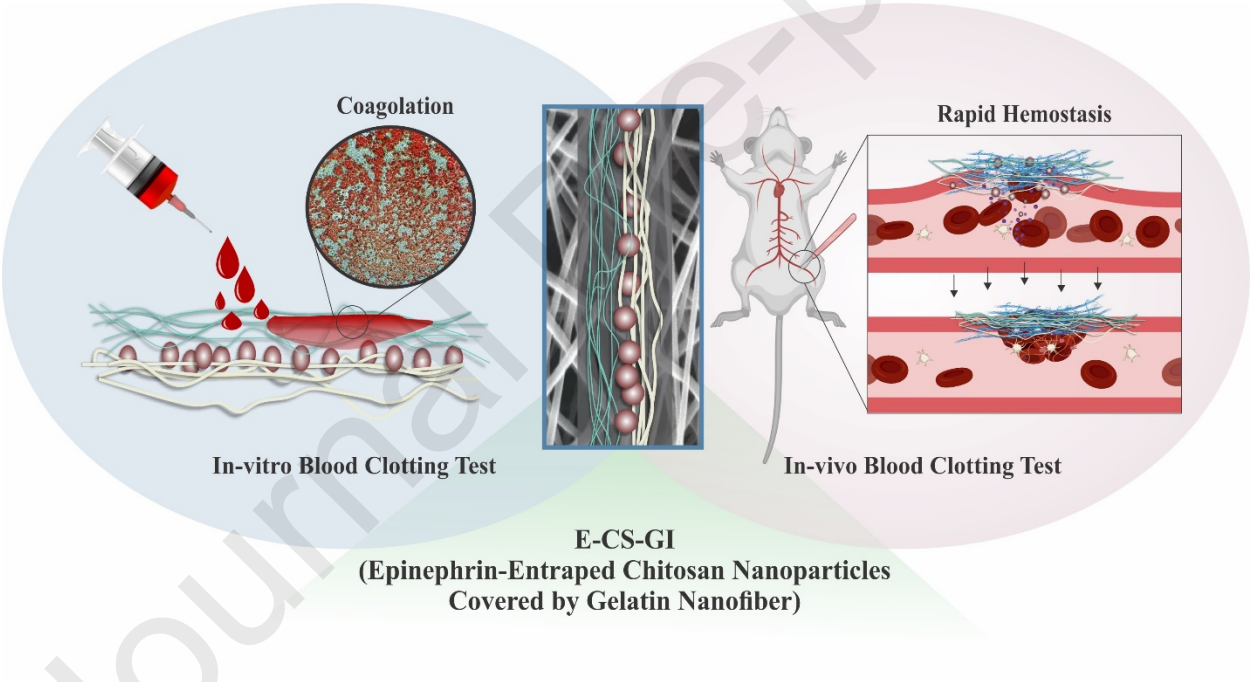

Declaration of interests

☒ The authors declare that they have no known competing financial interests or personal relationships that could have appeared to influence the work reported in this paper.

☐The authors declare the following financial interests/personal relationships which may be considered as potential competing interests: